



# YBa<sub>2</sub>Cu<sub>3</sub>O<sub>7</sub> films grown onto SrTiO<sub>3</sub> and YSZ substrates by chemical solution deposition of trifluoroacetates

A. Bustamante Domínguez<sup>1</sup> · L. De Los Santos Valladares<sup>2,3</sup> · H. Sanchez Cornejo<sup>1</sup> · A. M. Osorio-Anaya<sup>4</sup> · J. Flores Santibañez<sup>1</sup> · L. Sanchez Sovero<sup>1</sup> · C. H. W. Barnes<sup>2</sup>

Received: 17 June 2020 / Accepted: 11 July 2021 / Published online: 12 August 2021  
© The Author(s) 2021

## Abstract

We report the preparation and characterization of YBa<sub>2</sub>Cu<sub>3</sub>O<sub>7</sub> (YBCO) films grown onto SrTiO<sub>3</sub> and YSZ substrates by the trifluoroacetates chemical solution deposition method and following sintering with oxygen atmosphere at 860 °C. The X-ray diffraction (XRD) reveals (00 $\ell$ ) – oriented crystallites indicating epitaxial growth of the films in the *c*-direction. Despite granular morphology and the presence of Y<sub>2</sub>BaCuO<sub>5</sub> and CuO as minor secondary phases, the technique shows the successful formation of the superconducting YBCO and preventing the formation of the unwanted BaCO<sub>3</sub> phase. Rocking curve measurements of the (005) reflection for the YBCO/SrTiO<sub>3</sub> was fitted with one Gaussian function with full width at the half maximum (FWHM) of 0.44° confirming that it consists of YBCO crystallites with different texture. For the sample grown on YSZ, the rocking curve was fitted with two Gaussian functions, one corresponding to the YBCO layer (FWHM = 0.4°) and another to the substrate (FWHM = 0.3°). The magnetic measurements taken in zero field cooling and field cooling modes confirm the formation of the superconducting YBCO with critical temperatures (*T*<sub>C</sub>) 91.8 and 85.7 K for the samples grown onto YSZ and SrTiO<sub>3</sub>, respectively. The critical current density (*J*<sub>C</sub>) curves indirectly calculated by using the Bean's model from the *M*(*T*) loops were *J*<sub>C</sub> ~ 10<sup>9</sup> A/cm<sup>2</sup> for the sample deposited onto YSZ and *J*<sub>C</sub> ~ 10<sup>7</sup> A/cm<sup>2</sup> for the YBCO deposited onto SrTiO<sub>3</sub>. Overall, the difference in *T*<sub>C</sub> and *J*<sub>C</sub> values between both samples could be related to their difference in oxygen content, porosity, hole concentration per Cu ion and the presence of secondary phases.

**Keywords** YBCO · Chemical solution deposition · Superconductors · Trifluoroacetates

## 1 Introduction

The trifluoroacetate metal–organic chemical solution deposition (TFA-MO-CSD) method is a low cost route for producing YBCO superconducting films because it does not

require vacuum conditions or expensive equipment [1–13]. This technique was introduced by Gupta et al. in 1988 in order to prevent the formation of BaCO<sub>3</sub> [14–26] during fabrication of YBCO films by following the chemical solution deposition (CSD) method [27]. In fact, in other different CSD routes, BaCO<sub>3</sub> agglomerates at the grain boundaries affecting the critical current density (*J*<sub>C</sub>) of the resulting YBCO films up to a factor of around 10<sup>2</sup>–10<sup>3</sup> [28, 29]. The TFA-MO-CSD technique includes the preparation of the precursor solution by mixing Y and Ba trifluoro-acetates with Cu acetate (molar ratio 1:2:3) in methanol [30] or water [31]. The organic components are eliminated by pyrolysis at around 400 °C, yielding in Y<sub>2</sub>O<sub>3</sub>, BaF<sub>2</sub> and CuO. These intermediate compounds are then transformed into YBCO tetragonal (non superconductor) by annealing at around 800 °C. The YBCO orthorhombic (superconductor) phase is then obtained by oxygenating the latest compound at high temperatures. The drawback is that, by this technique, BaF<sub>2</sub> forms during the decomposition of the organic compounds

✉ L. De Los Santos Valladares  
ld301@cam.ac.uk; luisdv@mail.neu.edu.cn

<sup>1</sup> Laboratorio de Cerámicos Y Nanomateriales, Facultad de Ciencias Físicas, Universidad Nacional Mayor de San Marcos, Ap. Postal 14-0149, Lima 14, Perú  
<sup>2</sup> Cavendish Laboratory, Department of Physics, University of Cambridge, J.J. Thomson Ave, Cambridge CB3 0HE, UK  
<sup>3</sup> School of Materials Science and Engineering, Northeastern University, Shenyang 110819, Liaoning, China  
<sup>4</sup> Laboratorio de Nanotecnología E Innovación Tecnológica, Facultad de Química E Ingeniería Química, Universidad Nacional Mayor de San Marcos, Germán Amézaga 375, Lima, Perú

(pyrolysis) and the YBCO films are then obtained via hydrolysis of  $\text{BaF}_2$  [32].

About substrates,  $\text{SrTiO}_3$  and YSZ single crystals are commonly used to grow YBCO films since their lattice constant (0.3905 and 0.512 nm, respectively) are quite similar to that of YBCO orthorhombic. The mismatches with the YBCO lattice constant are: 1.35% for the  $\text{SrTiO}_3$  and 32.88% for the YSZ. However, these mismatches influence also in the morphology and magnetic properties of the resulting films [33]. We have previously reported the epitaxial growth of the YBCO film on YSZ substrate despite the highest mismatch in lattice constant with respect to YBCO [34].

In this work we grow YBCO onto  $\text{SrTiO}_3$  and YSZ substrates by following the TFA-MO-CSD method and sintering at 860 °C. We obtained uniaxial granular films showing superconducting behavior below ~90 K. The critical current density ( $J_C$ ) values of around  $10^5$  A/cm<sup>2</sup> was indirectly derived from the magnetic measurements using the Bean method. Overall, the difference in critical temperature ( $T_C$ ) and  $J_C$  values between both samples could be related to their difference in oxygen content, porosity, hole concentration per Cu ion and presence of secondary phases.

## 2 Experimental

The fabrication of the YBCO films was performed by the TFA-MO-CSD method and annealing. In this work, the following salts (99% purity, Alfa Aesar Inc.) were reacted: Y trifluoroacetate [ $\text{Y}(\text{OOCFF}_3)_3 \cdot 3-0 \text{ H}_2\text{O}$ ]; Cu trifluoroacetate (II) [ $\text{Cu}(\text{OOCFF}_3)_2 \cdot 0-7 \text{ H}_2\text{O}$ ] and Ba trifluoroacetate [ $\text{Ba}(\text{OOCFF}_3)_2 \cdot 1-9 \text{ H}_2\text{O}$ ]. Stoichiometric amounts of the Y:Ba:Cu trifluoroacetates in 1:2:3 ratio were mixed and completely dissolved in an ethanol ( $\text{C}_2\text{H}_5\text{OH}$ ) and bi-distilled water solution of 1:1 ratio using a magnetic stirrer at room temperature. Subsequently, the obtained solution containing the  $\text{Y}^{3+}$ ,  $\text{Cu}^{2+}$  and  $\text{Ba}^{2+}$  ions was decanted for 12 h in a matrix of oxalic acid and ethanol alcohol to obtain oxo-fluorates. The system was stirred at 250 rpm thereby to ensure a correct homogeneity. This precursor solution was directly dripped onto YSZ (100) and  $\text{SrTiO}_3$  (100) substrates using a Fisher pipette. The samples were immediately dried at 40 °C, in order to remove volatile elements. This process was repeated 7 times.

The crystallization and epitaxial growth of the YBCO layers were achieved by heat treatments and sintering at 860 °C in a tubular furnace (LENTON LTF-PTF Model 16/610) in oxygen atmosphere for 12<sup>h</sup>. Then, the furnace was set to 600 °C for 4<sup>h</sup> in oxygen atmosphere. The furnace was programmed to anneal and to quench the sample at the same ratio (1 °C/min).

The crystallization of the sample was studied by X-ray diffraction (XRD). The data were collected from 8° to 80° (0.02°

step) using a universal diffractometer Bruker D8 with Lynx Eye detector and  $\text{Cu K}_\alpha$  radiation ( $\lambda = 1.54,184 \text{ \AA}$ ). The morphology of the samples were inspected by scanning electron microscopy (SEM), cross sectional – transmission electron microscopy (CS-TEM) and high resolution-transmission electron microscopy (HR-TEM). For the TEM measurements the samples were coated with a Pt protective layer, then milled and thinned with a focused ion beam (FIB) in a dual-beam Quanta 3D apparatus (Philips). The interfaces were inspected in a Tecnai 20 (Philips) microscope, with a 200 keV beam generated by a tungsten source.

The superconducting state of the sample was studied from its susceptibility vs. temperature response which was obtained in a DC magnetic property measurement system (DC-MPMS—SQUID) from Quantum Design Inc. The data were collected in zero field cooling (ZFC) and field cooling (FC) modes in the temperature range 8—110 K. The critical current density ( $J_C$ ) for the samples were indirectly obtained from their respective hysteresis loops taken at 10 and 20 K by following the Bean's equation [35]:

$$J_C = \left[ \frac{20\Delta M}{tw^2 \left( l - \frac{w}{3} \right)} \right] \quad (1)$$

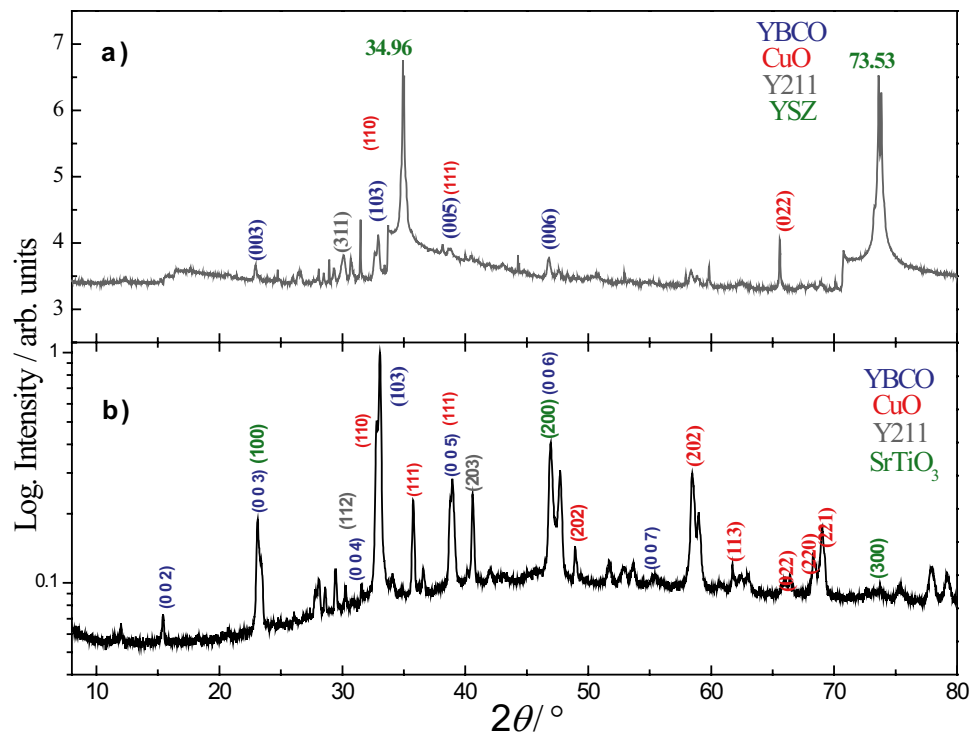
where  $\Delta M$  is the difference in magnetization values ( $+M$  and  $-M$ ) at a particular magnetic field; and  $t$ ,  $w$ , and  $l$  are the thickness, width and length of the samples, respectively.

## 3 Results and discussions

Figure 1 shows the X-ray diffraction, at logarithmical scale, of the annealed YBCO films. The presence of the peaks (003), (005) and (006) reveal epitaxial growth in the  $c$ -direction. The presence of the (103) reflection accounts for a minor part of YBCO that has not followed an epitaxial growth that possibly belonging to the most superficial layers of the sample. For the sample grown on YSZ, the two strong reflections at 34.96° and 73.53° correspond to the substrate. The first reflection screens the main (005) peak belonging to the YBCO film. The  $\text{Y}_2\text{BaCuO}_5$  (Y211) and CuO are also detected as secondary phases. The Y211 phase (PDF card 78–1719 [36]) is detected by the reflection around 29.99° corresponding to (311) peak. The CuO phase (PDF card 89–2899 [36]) might be present due to inhomogeneities in the starting precursor solution. This phase is observed in relative low intensity with reflections around 32.65° (110), 38.68° (111) and 65.57° (022).

For the case of the YBCO film grown onto  $\text{SrTiO}_3$  substrate, the XRD (Fig. 1(b)) shows the presence of the peaks (002), (003), (004), (005), (006) and (007) revealing epitaxial growth in the  $c$ -direction or the texture axis. The three

**Fig. 1** XRD pattern (in logarithmical scale) for the YBCO film grown onto YSZ (a) and SrTiO<sub>3</sub> (b) substrates by following the trifluoroacetate metal–organic chemical solution deposition method and annealing at 860 °C



strong reflections at 23.06°, 46.95° and 72.83° correspond to the SrTiO<sub>3</sub> substrate. The Y211 and CuO are also detected as secondary phases. A relative high number of CuO reflections are observed due to the low annealing temperature.

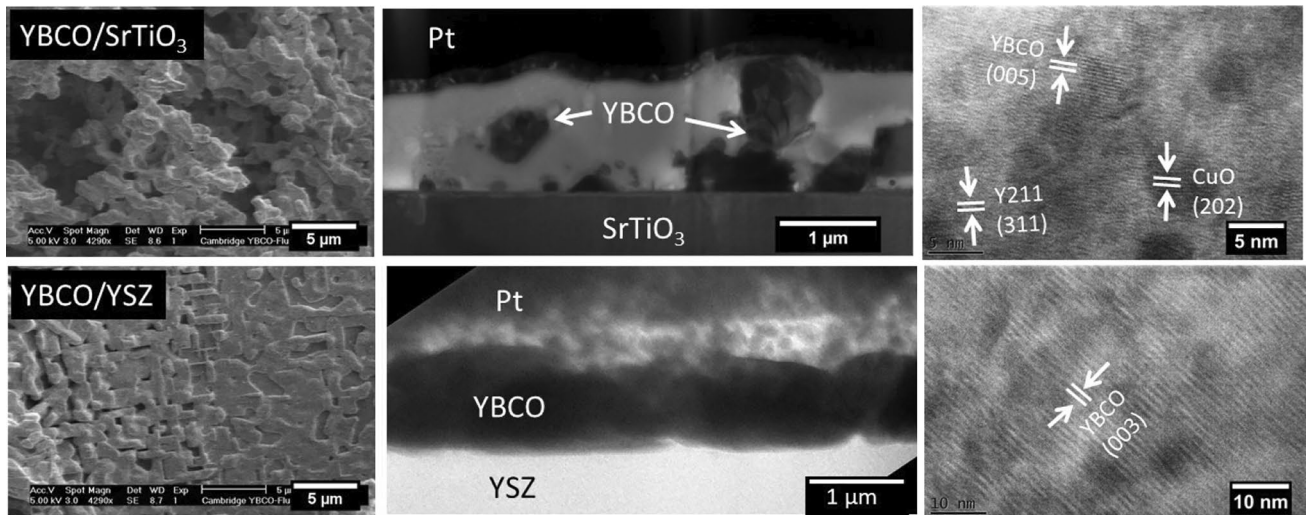
In general, the XRD patterns show a uniaxial texture along *c*-axis for the YBCO films growth in both substrates with no formation of BaCO<sub>3</sub> as secondary phase, proving the versatility of the TFA-CSD technique. The obtained phases, main reflections and crystalline parameters are listed in Table 1. For the case of the YBCO/YSZ sample, the phase has a relative high crystallite size (27.74 nm) compared to the secondary phases CuO and Y211 (23.84 and 22.28 nm respectively), while for the YBCO film grown onto SrTiO<sub>3</sub> substrate the highest crystallite size detected belongs to the CuO secondary phase (49.62 nm) and the minor size (35.23 nm) belongs to the YBCO superconductor phase. These differences might be related to the granularity of the films as discussed next in the microscopy analysis. Overall, these values confirm the versatility of the TFA-MO-CSD method for growing YBCO films [37, 38].

Figure 2 shows the surface morphology, cross sectional view and high resolution TEM images of the YBCO samples. As shown, the morphology of the films is granular, especially in the sample grown onto SrTiO<sub>3</sub>, in which agglomeration of grains is observed. In contrast, the sample grown onto YSZ substrate is more compact. The cross-sectional views indicate cumulus of YBCO grains together with unreacted phases. As mentioned in the experimental section, the top Pt layers were used for protecting the samples during FIB milling and do not influence in the morphology of the samples. Note that

the grain components in the sample grown on SrTiO<sub>3</sub> are not uniform and produce accumulation of around 1 μm size while for the sample grown on YSZ the film is more uniform

**Table 1** Phase formation, Miller indexes, peak positions, interplanar distances and crystallite sizes of YBCO thin films grown onto YSZ and SrTiO<sub>3</sub> substrates by following the TFA-MO-CSD technique and annealing at 860 °C

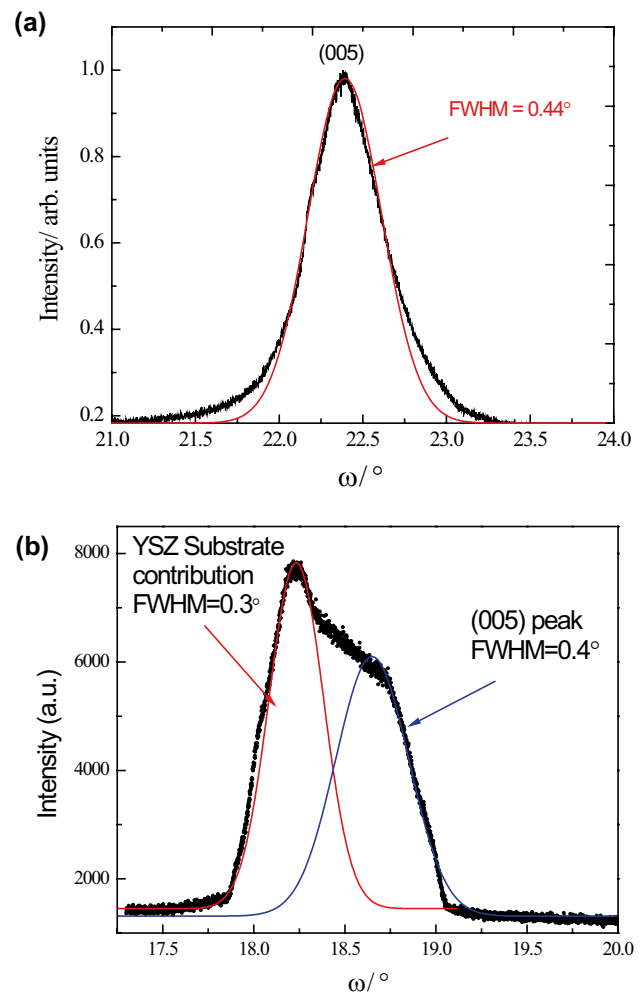
Substrate	Phase	Miller index	2 θ (°)	Interplanar distance (nm)	Crystallite sizes (nm)	
YSZ	YBCO	(003)	22.93	3.9	27.74	
		(103)	32.91	2.7		
		(005)	38.71	2.3		
		(006)	46.86	1.9		
	CuO	(110)	32.6	2.7	23.84	
		(111)	38.68	2.3		
		(022)	65.57	1.4		
	SrTiO <sub>3</sub>	Y211	(311)	29.99	2.9	22.28
		YBCO	(002)	15.46	5.8	35.23
			(003)	23.11	3.9	
(004)			30.79	2.9		
(103)			33.03	2.7		
(005)			38.91	2.3		
(006)			46.91	1.9		
(007)			55.39	1.6		
Y211		(112)	30.81	2.9	47.55	
CuO		(203)	40.61	2.2	49.62	
	(111)	35.73	2.5			
	(202)	48.91	1.7			
	(202)	58.43	1.6			
	(113)	61.71	1.5			
	(022)	65.99	1.5			
(220)	68.29	1.4				
(221)	69.01	1.4				



**Fig. 2** Surface, cross sectional TEM and high resolution TEM images of the YBCO films grown onto SrTiO<sub>3</sub> and YSZ substrates following the TFA-MO-CSD technique

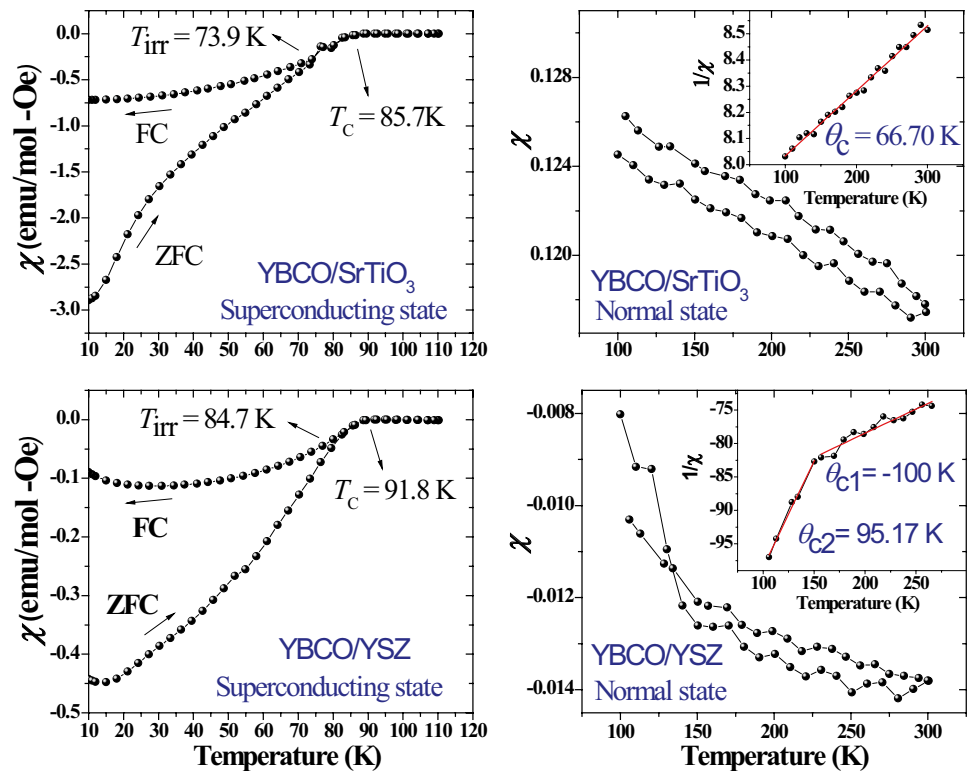
and compact. The HR-TEM image of the YBCO grains indicates crystallites of YBCO with interplanar distance 2.3 Å belonging to the (005) reflection, in agreement to the XRD and Table 1. For the YBCO/SrTiO<sub>3</sub> sample, the interplanar distances 2.9 and 1.7 nm are also observed corresponding to the Y211 (311) and CuO (202) reflections of the secondary phase. Thus, the YBCO film is highly granular and composed mainly by secondary phases, as it was also detected by the XRD above. Note that the sample grown onto YSZ is more compact and uniform showing an interplanar distance around 3.8 Å corresponding to the (003) reflection of the YBCO phase. These results suggest that 860 °C is not enough to form uniform YBCO film and leave unreacted phases Y211 and CuO (as also observed in the XRD plot).

In order to study the out-of-plane texture quality produced by the difference in substrates, Rocking Curve (RC) measurements were performed around the (005) reflection (Fig. 3). This reflection was chosen because its intensity is higher than the other (001) reflections and also because usually its position in the XRD plot (around  $2\theta = 38.72^\circ$ ) is far away from any other reflection from the substrate [33, 34]. However, as it is observed in Fig. 1(b), the YSZ reflection (around  $34.96^\circ$ ) is close to the (005) YBCO reflection. Thus, in order to maintain the same peak for the later comparison, we add the YSZ reflection's texture to the final fitting. The full width at the half maximum (FWHM) value of the RC provides information about the degree of inclination of the *c*-axes of the superconducting grains respecting to the normal axis to the substrate [39]. The RC measurement allows us to observe one region with out-of-plane texture for the YBCO/SrTiO<sub>3</sub> sample (see Fig. 3(a)), with FWHM ( $\Delta\omega$ ) = 0.44°. Similarly, Fig. 3(b) shows one region of texture with  $\Delta\omega = 0.40^\circ$  for de YBCO/YSZ sample. The observed substrate contribution suggests that, in contrast



**Fig. 3** Rocking curve measurement of the (005) YBCO reflection for (a) the YBCO/SrTiO<sub>3</sub> fitted with a Gaussian function with FWHM = 0.44° and (b) the YBCO/YSZ film where the contribution of the YSZ substrate is observed

**Fig. 4** Susceptibility vs temperature of YBCO films grown onto SrTiO<sub>3</sub> and YSZ substrates measured under an external magnetic field  $H_{\text{ext}} = 1$  kOe in the superconducting state (left) and in the normal state (right). Their onset transition temperature values  $T_{C(\text{onset})}$  are 85.7 K and 91.8 K, respectively



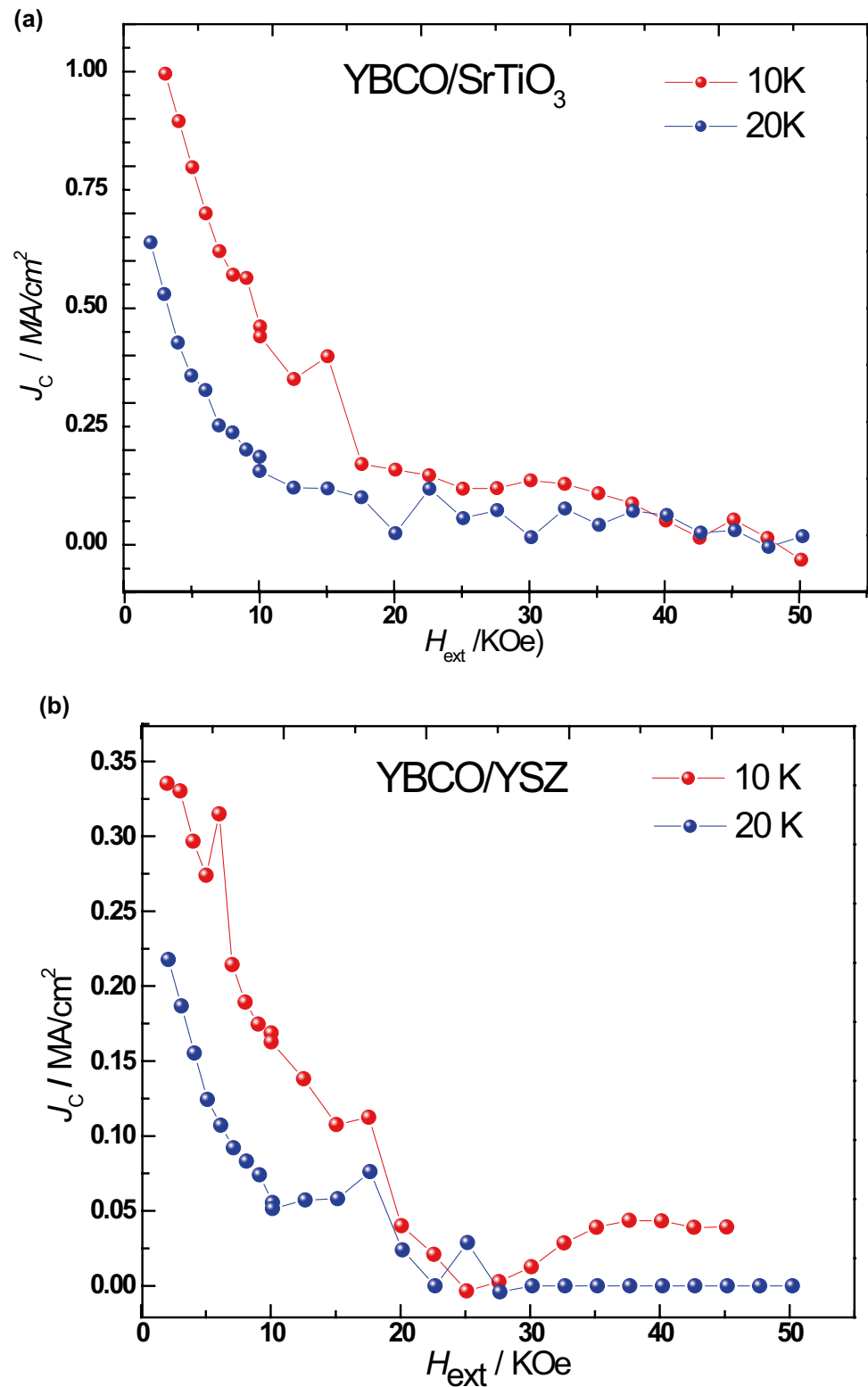
to the YBCO/SrTiO<sub>3</sub>, this film is in more contact with the substrate as confirmed by the cross sectional TEM images above; this in spite the greater lattice constant mismatch of the crystalline structure (32.88%) compared with the SrTiO<sub>3</sub> perovskite structure (1.35%) mentioned above. This effect might be also related to the differences in roughness in both substrate surfaces. To name, the YSZ surface is less rough than that for SrTiO<sub>3</sub>. The (005) YBCO peak is close to the YSZ (002) reflection (around 34.86°).

Figure 4 shows the temperature dependence of the susceptibility ( $\chi$ ) of the samples in the superconducting and normal states obtained under an applied magnetic field of 1 kOe. For the sample grown onto SrTiO<sub>3</sub>, it becomes diamagnetic (indicating the Meissner effect, typical from superconductors) from the onset temperature  $T_{C(\text{onset})} \approx 85.7$  K (see Fig. 4(a)). The point from which the ZFC and FC loops diverge define the irreversibility temperature ( $T_{\text{irr}}$ ) and it depends on the magnitude of the external magnetic field [38, 40]. Thus, under the applied magnetic field of 1 kOe,  $T_{\text{irr}} \approx 73.9$  K for the YBCO/SrTiO<sub>3</sub> sample. The corresponding  $\chi$  (T) loops in the normal state show weak ferromagnetic interaction between moments with Curie–Weiss temperature of  $\theta_C = 66.70$  K. Similarly, the susceptibility vs temperature plot for the sample grown on YSZ substrate reveals transition temperature values of  $T_{C(\text{onset})} \approx 91.8$  K and  $T_{\text{irr}} \approx 84.7$  K. Note that in this case, the inset  $1/\chi$  Vs. T plot is fitted with two lines suggesting the presence of two kind of magnetic interactions between moments: One

weak ferromagnetic interaction  $\theta_{C1} = 95.17$  K and another antiferromagnetic interaction with  $\theta_{C2} = -100$  K, being this last signal possibly caused due to other phases which are present in the sample.

Figure 5(a), (b) show the  $J_C(H)$  curves indirectly obtained by using the Bean's equation (Eq. 1) and the hysteresis loops taken at 10 and 20 K. For the sample YBCO/SrTiO<sub>3</sub>, the value of  $J_C$  (at  $H = 0$  Oe and  $T = 20$  K) is estimated as 0.9 MA/cm<sup>2</sup>. Whereas for the YBCO/YSZ,  $J_C$  (at  $H = 0$  Oe and  $T = 10$  K) is estimated as 0.36 MA/cm<sup>2</sup>. Table 2 compares the  $J_C$  values obtained in this work and those reported in the literature. According to it, the values of  $J_C$  seem to be influenced by the amount of different types of formed phases [7], the substrate and the growth temperature. High  $J_C$  values are obtained for the samples with less secondary phases and substrates with less lattice mismatch compared to that of YBCO [33]. Since the growth temperature mainly influences in the phase formation, density and epitaxy of the film, it should be adjusted depending on the used ingredients and type of substrates to obtain the highest  $J_C$  values. In addition to the secondary phases, the granularity and pores should also influence in the  $J_C$  values since they are obstacles for the transport of current [29]. This is observed in our results, the samples grown on SrTiO<sub>3</sub> presents greater  $J_C$  than over YSZ substrates. A lower degree of inclination also allows obtaining higher  $J_C$  values because the CuO<sub>2</sub> planes are better ordered along *ab*-plane. In the present work, a relative lower degree of

**Fig. 5** Critical current density curves obtained from the  $M(H)$  measurements by using the Bean's equation for the YBCO film on  $\text{SrTiO}_3$  (a) and YBCO film on YSZ (b)



inclination is observed in the YBCO/YSZ sample. Finally, considering that Y211 phase acts as flux pinning centers [33], the quantity of green phase also influences on the  $J_C$

values and according to the XRD patterns, a major quantity of Y211 reflections are observed in the (203) reflection around  $40.61^\circ$ .

**Table 2** Critical current density  $J_C$  values obtained at  $H_{ext}=0$  in this work and compared with those reported in the literature

Fabrication technique	$J_C$	$T_{growth}$ (K)	substrate	Secondary phases	Ref
CSD	$1 \times 10^6 \text{ Acm}^{-2}$ at 77 K	790 °C	LaAlO <sub>3</sub>	BaCuO <sub>2</sub> , CuO	[7]
CSD	$5 \times 10^5 \text{ Acm}^{-2}$ at 77 K	750 °C	LaAlO <sub>3</sub>	BaCuO <sub>2</sub> , CuO	[7]
TFA-MOD-CSD	$0.3 \times 10^9 \text{ A/cm}^2$ at 77 K	800 °C	LaAlO <sub>3</sub>	CuO, BaF <sub>2</sub> , Y <sub>2</sub> O <sub>3</sub>	[29]
TFA-MOD-CSD	$2.5 \times 10^9 \text{ A/cm}^2$ at 77 K	800 °C	LaAlO <sub>3</sub>	CuO, BaF <sub>2</sub> , Y <sub>2</sub> O <sub>3</sub>	[29]
TFA-MOD	$2.5 \times 10^6 \text{ Acm}^{-2}$ at 77 K	750 °C	CeO <sub>2</sub> /YSZ (IBAD)	BaCeO <sub>2</sub>	[41]
TFA-MOD-CSD	$1.5 \times 10^6 \text{ A/cm}^2$ at 10 K	860 °C	SrTiO <sub>3</sub>	CuO, Y211	This work
TFA-MOD-CSD	$0.9 \times 10^6 \text{ A/cm}^2$ at 20 K	860 °C	SrTiO <sub>3</sub>	CuO, Y211, YBa <sub>2</sub> Cu <sub>3</sub> O <sub>6</sub>	This work
TFA-MOD-CSD	$0.4 \times 10^6 \text{ A/cm}^2$ at 10 K	860 °C	YSZ	CuO, Y211, YBa <sub>2</sub> Cu <sub>3</sub> O <sub>6</sub>	This work
TFA-MOD-CSD	$0.3 \times 10^6 \text{ A/cm}^2$ at 20 K	860 °C	YSZ	CuO, Y211, YBa <sub>2</sub> Cu <sub>3</sub> O <sub>6</sub>	This work

## 4 Conclusions

YBCO films were successfully deposited on SrTiO<sub>3</sub> and YSZ single-crystal substrates via the trifluoroacetates metal–organic chemical solution deposition route and annealing at 860 °C. XRD revealed that most of the YBCO is *c*-axis oriented and without the formation of unwanted BaCO<sub>3</sub>. Rocking curves measurements shown only one out-of-plane textured region in both samples. The critical temperature values were 91.8 K and 85.7 K, corresponding to the YBCO samples grown on YSZ and SrTiO<sub>3</sub>, respectively. The difference in  $T_C$  values should be related to the oxygen content, the hole concentration per Cu ion and the presence of secondary phases. The  $J_C$  curves indirectly calculated by using the Bean's model from the  $M(H)$  loops were  $J_C \sim 10^9 \text{ A/cm}^2$  for the sample deposited on YSZ and  $J_C \sim 10^7 \text{ A/cm}^2$  for the YBCO/SrTiO<sub>3</sub> film being this difference product of the quantity of Y211 phase observed in XRD and also due to porosity and growth texture in the samples.

**Acknowledgements** This work was supported by the *Proyectos Integrales* Program from the CONCYTEC agency, project title “Fabricación de placas superconductoras de YBa<sub>2</sub>Cu<sub>3</sub>O<sub>7</sub>” (Contract No. 018-2020 – FONDECYT – BM). A Bustamante Domínguez and A. Osorio Anaya thank the Vice-Rector Office for Research and Postgraduate from the Universidad Nacional Mayor de San Marcos for supporting their projects **B151301031** and **B171301856**.

**Data availability** Data will be made available on reasonable request.

**Open Access** This article is licensed under a Creative Commons Attribution 4.0 International License, which permits use, sharing, adaptation, distribution and reproduction in any medium or format, as long as you give appropriate credit to the original author(s) and the source, provide a link to the Creative Commons licence, and indicate if changes were made. The images or other third party material in this article are included in the article's Creative Commons licence, unless indicated otherwise in a credit line to the material. If material is not included in the article's Creative Commons licence and your intended use is not permitted by statutory regulation or exceeds the permitted use, you will need to obtain permission directly from the copyright holder. To view a copy of this licence, visit <http://creativecommons.org/licenses/by/4.0/>.

## References

1. M.E. Gross, M. Hong, S.H. Liou, P.K. Gallagher, J. Kwo, Versatile. New Metalorganic Process for Preparing Superconducting Thin Films. *Appl. Phys. Lett.* **52**, 160–162 (1988)
2. M.L. Kullberg, M.T. Lanagan, W. Wu, R.B. Poeppel, A Sol-Gel Method for Preparing Oriented YBa<sub>2</sub>Cu<sub>3</sub>O<sub>7-x</sub> Films on Silver Substrates. *Supercond. Sci. Technol.* **4**, 337–342 (1989)
3. Y.L. Chen, J.V. Mantese, A.H. Hamdi, A.L. Mecheli, Microstructure and superconducting properties of Y-Ba-Cu-O and Yb-Ba-Cu-O thin films formed bby metalorganic deposition. *J. Mater. Res.* **4**, 1065–1070 (1989)
4. K. Yamagiwa, H. Hiei, Y. Takahashi, S.B. Kim, K. Matsumoto, H. Ikuta, U. Mizutani, I. Hirabayashi, Preparation of bi-axially aligned YBa<sub>2</sub>Cu<sub>3</sub>O<sub>7-δ</sub> film on CeO<sub>2</sub>-buffered MgO by chemical solution deposition. *Physica. C* **334**, 301–305 (2000)
5. P.C. McIntyre, M.J. Cima, J.A. Smith, R.B. Hallock, M.P. Siegal, J.M. Phillips, Effect of growth conditions on the properties and morphology of chemically derived epitaxial thin films of Ba<sub>2</sub>Y-Cu<sub>3</sub>O<sub>7-x</sub> on (001)LaAlO<sub>3</sub>. *J. Appl. Phys.* **71**, 1868–1877 (1992)
6. A. Malozemoff, S. Annavarapu, L. Fritzmeier, Q. Li, V. Prunier, M. Rupich, C. Thieme, W. Zhang, A. Goyal, M. Paranthaman, D.F. Lee, “Low-cost YBCO coated conductor technology”. *Supercond. Sci. Technol.* **13**, 473–476 (2000)
7. Oscar Castaño Linares, Síntesis y caracterización de capas delgadas superconductoras de altas corrientes críticas de YBa<sub>2</sub>Cu<sub>3</sub>O<sub>7</sub> obtenidas por MOD. Doctoral Thesis, Universitat autonoma de Barcelona. (2004)
8. X. Obradors, T. Puig, S. Ricart et al., Growth, nanostructure and vortex pinning in superconducting YBa<sub>2</sub>Cu<sub>3</sub>O<sub>7</sub> thin films based on trifluoroacetate solutions. *Supercond. Sci. Technol.* **25**, 123001 (2012)
9. M. Coll Bau, Chemical Solution Deposition of Oxide Buffer and Superconducting Layers for YBa<sub>2</sub>Cu<sub>3</sub>O<sub>7</sub> Coated Conductors. Doctoral thesis, Universidad Autónoma de Barcelona (2006)
10. X. Tang, Development of a fluorine-free chemical solution deposition route for rare-earth cuprate superconductor tapes and its application to reel-to-reel processing. Doctoral thesis Technical University of Denmark. (2008)
11. N.M. Alford, S.J. Penn, T.W. Button, High-temperature superconducting thick films. *Supercond. Sci. Technol.* **10**, 169–185 (1997)
12. T. Araki, I. Hirabayashi, Review of a Chemical Approach to YBa<sub>2</sub>Cu<sub>3</sub>O<sub>7-x</sub> Coated Superconductors—Metalorganic Deposition Using Trifluoroacetates. *Supercond. Sci. Technol.* **16**, R71-R94 (2003)
13. S. Morlens, N. Roma, S. Ricart, J.M. Moreto, T. Puig, A. Pomar, X. Obrador, Use of polymeric compounds to produce thick YBCO

- films by TFA-MOD process. *J. Phys: Conf. Ser.* **43**, 182–186 (2006)
14. H. Nonaka, S. Ichimura, T. Shimizu, K. Arai, Development of Oxidation Sources in Preparation of High-Tc Oxide Superconductor Thin Films Using the Molecular Beam Epitaxy Method. *Crit. Rev. Solid State Mater. Sci.* **20**, 285–338 (1995)
  15. L.C. Pathak, S.K. Mishra, A review on the synthesis of Y-Ba-Cu-oxide powder. *Supercond. Sci. Technol.* **18**, R67–R89 (2005)
  16. J.C. González, J.W. Flores, L. De Los Santos Valladares, A. Bustamante Domínguez, Correlation of puckered  $\text{CuO}_2$  superconducting planes with the superconducting critical temperature. *Rev. Soc. Quím. Perú* **81**, 350–359 (2015)
  17. L. De Los Santos Valladares, A. Bustamante Domínguez, R. Bellido Quispe, W. Flores Santibañez, J. Albino Aguiar, C.H.W. Barnes, Y. Majima, The irreversibility line and Curie-Weiss temperature of the superconductor  $\text{LaCaBaCu}_{3-x}(\text{BO}_3)_x\text{O}_7$  with  $x=0.2$  and  $0.3$ . *Phys. Procedia* **36**, 254–359 (2012)
  18. A. Bustamante Domínguez, L. León Felix, J. Garcia, J. Flores Santibañez, L. De Los Santos Valladares, J.C. González, A. Osorio Anaya, M. Pillaca, Epitaxial growth of  $\text{YBa}_2\text{Cu}_3\text{O}_7$  films onto  $\text{LaAlO}_3$  (100) by using oxalates. *Phys. Procedia* **36**, 526–531 (2012)
  19. A. Bustamante Domínguez, L. De Los Santos Valladares, J. Flores Santibañez, C.H.W. Barnes, Y. Majima, Aging effect in  $\text{CaLaBaCu}\{\text{Cu}_{1-x}\text{Fe}_x\}_3\text{O}_{7-8}$  with  $0 \leq x \leq 0.07$  studied by Mössbauer spectroscopy. *Hyperfine Interact.* **203**, 119–124 (2011)
  20. L. De Los Santos Valladares, D. Angel Bustamante, J.C. Gonzalez, L. Juan Feijoo, A. Ana Osorio, T. Mitrelias, Y. Majima, C.H. Barnes, Magnetic properties of the superconductor  $\text{LaCaBaCu}_3\text{O}_7$ . *The Open Supercond. J.* **2**, 19–27 (2010) <https://doi.org/10.2174/1876537801002010019>
  21. L. De Los Santos Valladares, A.G. Bustamante Domínguez, J.C. Gonzalez González, J. Flores Santibañez, X. Obradors, Superconductivity in the System  $\text{CaLaBaCu}_{3-x}(\text{PO}_4)_x\text{O}_{7-8}$  with  $X=0.1, 0.3, 0.5$ . *J. Phys. Chem. Solid* **67**, 605–609 (2006)
  22. A. Bustamante Domínguez, L. De Los Santos Valladares, B.L. Willems, V.H. Barinotto, J.C. González González, X. Obradors, Superconductivity in the System  $[\text{Y}_{0.8}\text{Ca}_{0.2}](\text{SrBa})\text{Cu}_{3-x}(\text{BO}_3)_x\text{O}_{7-8}$  with  $X$ . *J. Phys. Chem. Solid* **67**, 594–596 (2006)
  23. A. Bustamante Domínguez, A.M. Osorio Anaya, L. De Los Santos Valladares, H. Carhuancho, J.C. González González, G. Cernicchiaro, J.A. Feijoo Levano, Synthesis of  $\text{YBa}_2\text{Cu}_3\text{O}_{7-8}$  using oxalate precursor and sol-gel method. *Adv. Sci. Tech.* **47**, 37–42 (2006)
  24. L. De Los Santos Valladares, A. Bustamante Domínguez, J. Flores Santibañez, J.C. González González, Preparation and characterization of the superconductor  $\text{CaLaBaCu}_{2.8}(\text{PO}_4)_{0.2}\text{O}_{6.2}$  compound. *Physica. C.* 408–410 44–45 (2004)
  25. A. Bustamante Domínguez, R. Bellido Quispe, L. De Los Santos Valladares, J. C. González, Preparation and characterization of the superconductor  $\text{CaLaBaCu}_{2.8}(\text{BO}_3)_{0.2}\text{O}_{6.4}$  Compound. *Physica. C.* 408–410 884–885 (2004)
  26. V.H. Barinotto Call-Cardenas, B.L. Willems, A.G. Bustamante Domínguez, L. De Los Santos Valladares, J.C. Gonzalez Gonzalez, Preparation and characterization of the superconductor  $[\text{Y}_{0.8}\text{Ca}_{0.2}]\text{SrBaCu}_{2.8}(\text{BO}_3)_{0.2}\text{O}_{6.4}$  compound. *G. Physica. C.* 408–410 58–59 (2004)
  27. A. Gupta, R. Jagannathan, E.I. Cooper, E.A. Giess, J.I. Landman, B.W. Hussey, Superconducting oxide films with high transition temperature prepared from metal trifluoroacetate precursors. *Appl. Phys. Lett.* **52**, 2077–2079 (1988)
  28. X. Obradors, T. Puig, A. Pomar, F. Sandiumenge, S. Piñol, N. Mestres, O. Castaño, M. Coll, A. Cavallaro, A. Palau, J. Gázquez, J.C. González, J. Gutierrez, N. Romá, S. Ricart, J.M. Moretó, M.D. Rossell, G. van Tendeloo, Chemical solution deposition: a path towards low cost coated conductors. *Supercond. Sci. Technol.* **17**, 1055–1064 (2004)
  29. J.C. Gonzalez. Coated conductors and chemical solution growth of YBCO films: A micro-Raman spectroscopy study. Doctoral thesis. Universitat Autonoma de Barcelona (2005)
  30. X.M. Cui, B.W. Tao, Z. Tian, J. Xiong, X.Z. Liu, Y.R. Li, YBCO thin films prepared by fluorine-reduced metal-organic deposition using trifluoroacetates. *Supercond. Sci. Technol.* **19**, L13–L15 (2006)
  31. S. Wang, L. Wang, B. Gu, High Quality YBCO Film Growth on  $\text{SrTiO}_3$ -Buffered  $\text{LaAlO}_3$  Substrate by Full Solution Method. *J. Mater. Sci. Technol.* **24**, 899–902 (2008)
  32. P.C. McIntyre, M.J. Cima, J.A. Smith, R.B. Hallock, M.P. Siegal, J.M. Phillips, Effect of growth conditions on the properties and morphology of chemically derived epitaxial thin films of  $\text{Ba}_2\text{YCu}_3\text{O}_{7-x}$  on (001)  $\text{LaAlO}_3$ . *J. Appl. Phys.* **71**, 1868–1877 (1992)
  33. L. De Los Santos Valladares, J.C. González, A. Bustamante Domínguez, A.M. Osorio Anaya, H. Sanchez Cornejo, S. Holmes, J. Albino Aguiar, C.H.W. Barnes, A fluorine-free oxalate route for the chemical solution deposition of  $\text{YBa}_2\text{Cu}_3\text{O}_7$  films in Superconductors, edited by Alexander Gabovich, ISBN 978–953–51–4163–1. Intech. Chapter 3, 35–53 (2015)
  34. H.E. Sanchez Cornejo, A. Bustamante Domínguez, A. M. Osorio, L. De Los Santos Valladares, J. Albino Aguiar, C.H.W. Barnes, Chemical solution deposition of  $\text{YBa}_2\text{Cu}_3\text{O}_7$  films on  $\text{YSZ}(100)$  substrates. *J. Chem. Chem. Eng.* **8**, 547–551 (2014)
  35. J. Narayan, A. Bhaumik y, R. Sachan, High temperature superconductivity in distinct phases of amorphous B-doped Q-carbon. *J. Appl. Phys.* **123**, 135304 (2018)
  36. Powder Diffraction File PCPDFWIN, Version 2.1 JCPDS, The International Centre for Diffraction Data (2000)
  37. Claudia Apetrii,  $\text{YBa}_2\text{Cu}_3\text{O}_{7-x}$  thin films prepared by Chemical Solution Deposition. Doctoral thesis, Technical University of Dresden (2009)
  38. L. De los Santos Valladares, A Bustamante Dominguez, R. Bellido Quispe, J.W. Flores, J. Albino Aguiar, C.H.W. Barnes, The irreversibility line and Curie-Weiss temperature of the superconductor  $\text{LaCaBaCu}_{3-x}(\text{BO}_3)_x$  with  $x=0.2$  and  $0.3$ . *Physics. Procedia* **36** 354–359 (2012)
  39. X. Obradors, T. Puig, S. Ricart, M. Coll, J. Gázquez, A. Palau, X. Granados, Growth, nanostructure and vortex pinning in superconducting  $\text{YBa}_2\text{Cu}_3\text{O}_7$  thin films based on trifluoroacetate solutions. *Supercond. Sci. Technol.* **25**(12), 123001 (2012). <https://doi.org/10.1088/0953-2048/25/12/123001>
  40. L. De Los Santos Valladares, H. Sanchez Cornejo, C.H.W. Barnes, N.O. Moreno, A. Bustamante Domínguez, Texture and magnetic anisotropy of  $\text{YBa}_2\text{Cu}_3\text{O}_{7-x}$  film on  $\text{MgO}$  substrate. *J. Mater. Sci. Mater. Electron.* **31**, 21108 – 21117 (2020)
  41. T. Araki, T. Yuasa, H. Kurosaki, Y. Yamada, I. Hirabayashi, T. Kato, T. Hirayama, Y. Lijima, T. Saito, High- $J_c$   $\text{YBa}_2\text{Cu}_3\text{O}_{7-x}$  films on metal tapes by the metalorganic deposition method using trifluoroacetates. *Supercond. Sci. Technol.* **15**, L1–L3 (2002)

**Publisher's Note** Springer Nature remains neutral with regard to jurisdictional claims in published maps and institutional affiliations.